Turkish J. Eng. Env. Sci.
26 (2002) , 403 – 418.

Steady Flow of a Walter's B' Viscoelastic Fluid between a Porous Elliptic Plate and the Ground

Serdar BARIŞ
University of İstanbul, Faculty of Engineering,
Department of Mechanical Engineering,
İstanbul-TURKEY

Received 23.10.2001

Abstract

Steady three-dimensional flow of a Walter's B' viscoelastic fluid between a porous elliptic plate and the ground was considered. From a practical point of view, this problem corresponds to fluid-cushioned porous sliders, which are useful in reducing the frictional resistance of moving objects. The basic equations governing the flow were reduced to a set of ordinary differential equations by using the appropriate transformations for the velocity components. Perturbation solutions of the velocity field were obtained by taking the cross-flow Reynolds number as the perturbation parameter. The graphical presentation of the results readily reveals the differences between the Newtonian and viscoelastic flow phenomena. In addition, with regard to optimum efficiency, it is shown that it is more advantageous to move an elliptic plate with high eccentricity along the major axis when a viscoelastic fluid is used.

Key words: Walter's B' viscoelastic fluid, Porous elliptic plate, Lift and drag.

Introduction

Within the past fifty years, there has been remarkable interest in the flow of Newtonian and non-Newtonian fluids through channels with porous walls owing to their applications in various branches of engineering and technology. Familiar examples are boundary layer control, transpiration cooling and gaseous diffusion. In addition, blowing is used to add reactants, prevent corrosion and reduce drag. Suction is applied to chemical processes to remove reactants. Much work has been done in order to understand the effects of fluid removal or injection through channel walls on the flow of Newtonian and non-Newtonian fluids. Berman (1953) made an initial effort in this direction. His investigations provided a technique for solving the classical viscous flow equations. Further contributions have been made since then by Sellars (1955), Yuan (1956), White *et al.* (1958), Proudman (1960), Terrill and Shrestha (1965), Skalak and Wang (1978), Brady (1984), Zaturska *et al.* (1988), and many others. We refer the reader to the studies by Cox (1991) and Choi *et al.* (1999), and references cited in the above-mentioned articles regarding detailed analysis of various results on this subject.

In this paper, we shall discuss the flow of a Walter's B' viscoelastic fluid between a porous elliptic plate and the ground. From a technological point of view, flows of this type correspond to porous sliders, which are becoming increasingly important due to their attractive performance and their application in fluid-cushioned moving pads. It is a well-known fact that fluid-cushioned porous sliders are useful in reducing the frictional resistance between two solid surfaces moving relative to each other. For Newtonian fluids, previous studies include the porous circular slider (Wang, 1974), the porous flat slider (Skalak and Wang, 1975), and the porous elliptic slider (Wang, 1978; Watson *et al.*, 1978). Later, for a second-order viscoelastic fluid, the fluid dynamics of a porous flat slider was studied by Bhatt (1981)

obtaining the first-order perturbation solution for the case of a very low cross-flow Reynolds number. However, Bhatt's results seem to be in error, as also pointed out by Ariel (1993). Recently, Ariel (1993) has extended Skalak and Wang's analysis (1975) to a Walter's B' viscoelastic fluid, which is characterized by two material constants. In his study, the perturbation and exact numerical solutions have been obtained.

While a great deal of work has been done on the flow between porous plates, it appears that very little attention has been paid to the three-dimensional flow cases where the fluids exhibit a non-Newtonian character. Therefore, the present paper aims to solve such a problem involving the porous elliptic slider by introducing a Walter's B' viscoelastic fluid and to assess qualitatively the effect of the elasticity of the fluid on the components of velocity, the axial pressure drop, lift and drag. The perturbation solutions in this paper include those given by Ariel (1993) as a special case, since our current results reduce to the flat case when the square of the ratio of the minor axis to the major axis (β) is equal to 0.

Constitutive equations

The inadequacy of the theory of Newtonian fluids in predicting the behaviour of some fluids, especially those with high molecular weight, leads to developments in non-Newtonian fluid mechanics. There are numerous models of viscoelastic fluids suggested in the literature. To get some insight into their flow behaviour, it is preferable to restrict oneself to a model with a minimum number of parameters in the constitutive equations. We chose the model of Walter's B' viscoelastic fluid for our study as it involves only one non-Newtonian parameter. The Cauchy stress tensor $\mathbf{T}$ in such a fluid is related to the motion in the following manner:

$$\mathbf{T} = -p\mathbf{I} + 2\eta_0\mathbf{e} - 2k_0\frac{\delta\mathbf{e}}{\delta t} \tag{1}$$

In this equation, p is the pressure, $\mathbf{I}$ is the identity tensor, and the rate of strain tensor $\mathbf{e}$ is defined by

$$2\mathbf{e} = \nabla\mathbf{v} + (\nabla\mathbf{v})^T \quad \{(\nabla\mathbf{v})^{ij} = \frac{\partial v_j}{\partial x_i}\}, \tag{2}$$

where $\mathbf{v}$ is the velocity vector, ∇ is the gradient operator, and $\delta/\delta t$ denotes the convected differentiation of a tensor quantity in relation to the material in motion. The convected differentiation of the rate of strain tensor is given by

$$\frac{\delta\mathbf{e}}{\delta t} = \frac{\partial\mathbf{e}}{\partial t} + \mathbf{v}\cdot\nabla\mathbf{e} - \mathbf{e}\cdot\nabla\mathbf{v} - (\nabla\mathbf{v})^T\cdot\mathbf{e} \tag{3}$$

Finally η_0 and k_0 are, respectively, the limiting viscosity at a small rate of shear and the short memory coefficient which are defined through

$$\eta_0 = \int_0^\infty N(\tau)d\tau, \quad k_0 = \int_0^\infty \tau N(\tau)d\tau, \tag{4}$$

where $N(\tau)$ is the distribution function with relaxation time τ. This idealized model is a valid approximation of Walter's B' viscoelastic fluid taking very short memory into account so that terms involving

$$\int_0^\infty \tau^n N(\tau)d\tau, \quad n \geqslant 2 \tag{5}$$

have been neglected. For a detailed description of this model the reader should consult Beard and Walters (1964).

Formulation of the problem

Figure 1 shows the physical model and coordinate system. A fluid is injected through an elliptic plate, the boundary of which is described by $x^2 + \beta y^2 = D^2(\beta < 1), z = d$, where β is the square of the ratio of the minor axis to the major axis. As in Wang's study (1978), the supply pressure is assumed to be large enough to cause a nearly constant injection velocity U_3 through the elliptic plate. The porous elliptic plate is moving laterally at velocities U_1 and U_2 along the negative x and y directions, respectively. We have further assumed the gap width d between the elliptic plate and the ground is small compared with D, i.e. D >> d. Due to this assumption the edge effects can be ignored.

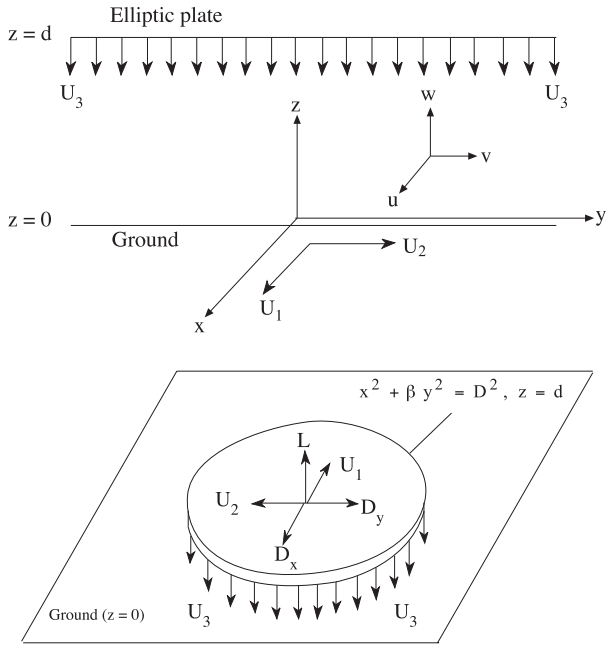

Figure 1. Sketch of flow geometry and coordinate system

In addition to Eq. (1), the basic equations of the problem are the following:

Continuity equation:

$$\nabla \cdot \mathbf{v} = 0, \tag{6}$$

Equations of motion:

$$\rho(\mathbf{v} \cdot \nabla \mathbf{v}) = \nabla \cdot \mathbf{T}, \tag{7}$$

where ρ is the density. The assumptions made in the above equations are as follows: (a) The flow is steady and laminar; (b) The fluid is incompressible; (c) The body forces are negligible.

Substituting the Cauchy stress tensor from Eq. (1) into equations of motion (7), with the aid of Eqs. (2) and (3), we get

$$\begin{aligned} \rho(\mathbf{v} \cdot \nabla \mathbf{v}) = \; & -\nabla p + \eta_0 \nabla^2 \mathbf{v} - 2k_0 \mathbf{v} \cdot \nabla \nabla^2 \mathbf{v} \\ & + k_0 \nabla^2 (\mathbf{v} \cdot \nabla \mathbf{v}). \end{aligned} \tag{8}$$

In a reference frame translating with the porous elliptic plate, let u, v, and w be the velocity components corresponding to the x, y and z directions, respectively. Following Wang (1978), we look for a solution, compatible with the continuity equation (6), of the form

$$\begin{aligned} & u = U_1 f(\eta) + \frac{U_3 x}{d} h'(\eta), v = U_2 g(\eta) + \frac{U_3 y}{d} k'(\eta), \\ & w = -U_3 \{h(\eta) + k(\eta)\}, \end{aligned} \tag{9}$$

where $\eta = z/d$ and the prime denotes the differentiation with respect to η.

The boundary conditions for the velocity field are

$$\begin{aligned} & u(0) = U_1, v(0) = U_2, w(0) = 0, u(1) = 0, \\ & v(1) = 0, w(1) = -U_3 \end{aligned} \tag{10}$$

By using equations of motion (8) and similarity transformation (9) it can be shown that the general expression for the pressure distribution is

$$\begin{aligned} p(x, y, \eta) = \; & C_1 y + C_3 x + C_2 \tfrac{y^2}{2} + C_4 \tfrac{x^2}{2} - \tfrac{1}{2}\rho w^2 \\ & + \eta_0 \tfrac{dw}{dz} + 2k_0 (\tfrac{dw}{dz})^2 - k_0 w \tfrac{d^2 w}{dz^2} + p_0, \end{aligned} \tag{11}$$

where the constants C_1, C_2, C_3 and C_4 are

$$\begin{aligned} C_1 = \; & \tfrac{\eta_0 U_2}{d^2} (g'' + R\{(h+k)g' - k'g\} \\ & + RN\{(h+k)g''' - (k' + 2h')g'' \\ & + (k'' - h'')g' - k'''g\}), \end{aligned} \tag{12}$$

$$\begin{aligned} C_2 = \; & \tfrac{\eta_0 U_3}{d^3} (k''' + R\{(h+k)k'' - k'^2\} \\ & + RN\{(h+k)k^{IV} - 2(h'+k')k''' \\ & - h''k'' + k''^2\}), \end{aligned} \tag{13}$$

$$\begin{aligned} C_3 = \; & \tfrac{\eta_0 U_1}{d^2} (f'' + R\{(h+k)f' - h'f\} \\ & + RN\{(h+k)f''' - (h' + 2k')f'' \\ & + (h'' - k'')f' - h'''f\}), \end{aligned} \tag{14}$$

$$\begin{aligned} C_4 = \; & \tfrac{\eta_0 U_3}{d^3} (h''' + R\{(h+k)h'' - h'^2\} \\ & + RN\{(h+k)h^{IV} - 2(h'+k')h''' \\ & - k''h'' + h''^2\}), \end{aligned} \tag{15}$$

and p_0 is the constant of integration. In the above equations, the cross-flow Reynolds number R and dimensionless measure of viscoelasticity of the fluid N are defined through, respectively

$$R = \frac{\rho U_3 d}{\eta_0}, \quad N = \frac{k_0}{\rho d^2}. \tag{16}$$

In view of the fact that the shape of the porous plate makes the isobars similar ellipses, the constants $C_1, ..., C_4$ must satisfy the following equations:

$$C_1 = 0, C_3 = 0, C_2 = \beta C_4 \tag{17}$$

Substituting Eq. (17) into Eqs. (11) – (15), we obtain

$$p(x, y, \eta) = \frac{\rho U_3^2 A}{2d^2 R}(x^2 + \beta y^2) - \frac{1}{2}\rho w^2 + \eta_0 \frac{dw}{dz} + 2k_0(\frac{dw}{dz})^2 - k_0 w \frac{d^2 w}{dz^2} + p_0, \tag{18}$$

$$h''' + R\{(h+k)h'' - h'^2\} + RN\{(h+k)h^{IV} - 2(h'+k')h''' - k''h'' + h''^2\} = A, \tag{19}$$

$$k''' + R\{(h+k)k'' - k'^2\} + RN\{(h+k)k^{IV} - 2(h'+k')k''' - h''k'' + k''^2\} = \beta A, \tag{20}$$

$$f'' + R\{(h+k)f' - h'f\} + RN\{(h+k)f''' - (h'+2k')f'' + (h''-k'')f' - h'''f\} = 0, \tag{21}$$

$$g'' + R\{(h+k)g' - k'g\} + RN\{(h+k)g''' - (k'+2h')g'' + (k''-h'')g' - k'''g\} = 0, \tag{22}$$

The boundary conditions on velocity given by Eq. (10) require

$$h(0) = h'(0) = h'(1) = 0, \quad k(0) = k'(0) = k'(1) = 0, \quad h(1) + k(1) = 1,$$

$$f(0) = 1, f(1) = 0, g(0) = 1, g(1) = 0. \tag{23}$$

It is recorded that for Newtonian fluid (N = 0) Eqs. (18) – (23) are the same as those obtained by Wang (1978).

Perturbation solution for small R

Equations (19) – (22) are a set of ordinary coupled nonlinear differential equations, the order of which exceeds the number of boundary conditions, and which are very difficult to integrate numerically, so we use a perturbation method to obtain an approximate solution for the velocity components. Here it is assumed that the cross-flow Reynolds number is very small; then $h(\eta), k(\eta), f(\eta), g(\eta)$ and A can be expanded in terms of the small parameter R:

$$\begin{aligned} h &= h_0 + Rh_1 + R^2 h_2 + ..., \\ k &= k_0 + Rk_1 + R^2 k_2 + ..., \\ f &= f_0 + Rf_1 + R^2 f_2 + ..., \\ g &= g_0 + Rg_1 + R^2 g_2 + ..., \\ A &= A_0 + RA_1 + R^2 A_2 + ..., \end{aligned} \tag{24}$$

where $h_n's, k_n's, f_n's, g_n's$ and A are independent of R. Inserting Eqs. (24) into Eqs. (19) – (22) and equating the coefficients of different powers of R to zero, we get the system of differential equations

$$h_0''' = A_0, k_0''' = \beta A_0, f_0'' = 0, g_0'' = 0, \tag{25}$$

$$h_1''' + (h_0 + k_0)h_0'' - h_0'^2 + N\{(h_0 + k_0)h_0^{IV} - 2(h_0' + k_0')h_0''' - k_0''h_0'' + h_0''^2\} = A_1, \tag{26}$$

$$k_1''' + (h_0 + k_0)k_0'' - k_0'^2 + N\{(h_0 + k_0)k_0^{IV} - 2(h_0' + k_0')k_0''' - h_0''k_0'' + k_0''^2\} = \beta A_1, \tag{27}$$

$$f_1'' + (h_0 + k_0)f_0' - h_0'f_0 + N\{(h_0 + k_0)f_0''' - (h_0' + 2k_0')f_0'' + (h_0'' - k_0'')f_0' - h_0'''f_0\} = 0, \tag{28}$$

$$g_1'' + (h_0 + k_0)g_0' - k_0'g_0 + N\{(h_0 + k_0)g_0''' - (k_0' + 2h_0')g_0'' + (k_0'' - h_0'')g_0' - k_0'''g_0\} = 0, \tag{29}$$

$$h_2''' + (h_1 + k_1)h_0'' + (h_0 + k_0)h_1'' - 2h_0'h_1' + N\{(h_1 + k_1)h_0^{IV} + (h_0 + k_0)h_1^{IV}$$

$$-2(h_1' + k_1')h_0''' - 2(h_0' + k_0')h_1''' + (2h_1'' - k_1'')h_0'' - k_0''h_1''\} = A_2, \tag{30}$$

$$k_2''' + (h_1 + k_1)k_0'' + (h_0 + k_0)k_1'' - 2k_0'k_1' + N\{(h_1 + k_1)k_0^{IV} + (h_0 + k_0)k_1^{IV}$$

$$-2(h_1' + k_1')k_0''' - 2(h_0' + k_0')k_1''' + (2k_1'' - h_1'')k_0'' - h_0''k_1''\} = \beta A_2, \tag{31}$$

$$f_2'' + (h_1 + k_1)f_0' + (h_0 + k_0)f_1' - h_1'f_0 - h_0'f_1 + N\{(h_1 + k_1)f_0''' + (h_0 + k_0)f_1'''$$

$$-(h_1' + 2k_1')f_0'' - (h_0' + 2k_0')f_1'' + (h_1'' - k_1'')f_0' + (h_0'' - k_0'')f_1' - h_1'''f_0 - h_0'''f_1\} = 0, \tag{32}$$

$$g_2'' + (h_1 + k_1)g_0' + (h_0 + k_0)g_1' - k_1'g_0 - k_0'g_1 + N\{(h_1 + k_1)g_0''' + (h_0 + k_0)g_1'''$$

$$-(k_1' + 2h_1')g_0'' - (k_0' + 2h_0')g_1'' + (k_1'' - h_1'')g_0' + (k_0'' - h_0'')g_1' - k_1'''g_0 - k_0'''g_1\} = 0, \tag{33}$$

The boundary conditions (23) are re-written as follows:

$$h_n(0) = 0, h_n'(0) = 0, h_n'(1) = 0, k_n(0) = 0, k_n'(0) = 0, k_n'(1) = 0,$$

$$h_0(1) + k_0(1) = 1, h_m(1) + k_m(1) = 0, f_0(0) = 1, f_n(1) = 0, f_m(0) = 0,$$

$$g_0(0) = 1, g_n(1) = 0, g_m(0) = 0, (n = 0, 1, 2; m = 1, 2) \tag{34}$$

Integrating Eqs. (25) – (33) with the boundary conditions (34), we have

Zeroth-order solution:

$$h_0 = \frac{3\eta^2 - 2\eta^3}{1+\beta}, k_0 = \frac{\beta(3\eta^2 - 2\eta^3)}{1+\beta}, f_0 = 1-\eta, g_0 = 1-\eta, \tag{35}$$

First-order solution:

$$h_1 = \frac{16 + (84N-1)\beta + (37-420N)\beta^2}{70(1+\beta)^3}\eta^2 + \frac{-27 + (504N-18)\beta + (840N-27)\beta^2}{70(1+\beta)^3}\eta^3$$

$$-\frac{12N\beta}{(1+\beta)^2}\eta^4 + \frac{3(1-\beta+16N)}{10(1+\beta)^2}\eta^5 + \frac{2\beta-1}{5(1+\beta)^2}\eta^6 + \frac{2(1-2\beta)}{35(1+\beta)^2}\eta^7, \tag{36}$$

$$k_1 = \frac{(37-420N)\beta + (84N-1)\beta^2 + 16\beta^3}{70(1+\beta)^3}\eta^2 + \frac{(840N-27)\beta + (504N-18)\beta^2 - 27\beta^3}{70(1+\beta)^3}\eta^3$$

$$-\frac{12N\beta}{(1+\beta)^2}\eta^4 + \frac{3\beta(\beta-1+16N)}{10(1+\beta)^2}\eta^5 + \frac{\beta(2-\beta)}{5(1+\beta)^2}\eta^6 + \frac{2\beta(\beta-2)}{35(1+\beta)^2}\eta^7, \tag{37}$$

$$f_1 = \frac{(20N-3)(3+\beta)}{20(1+\beta)}\eta - 3N\eta^2 + \frac{1+2N\beta}{1+\beta}\eta^3 + \frac{\beta-3}{4(1+\beta)}\eta^4 + \frac{2-\beta}{10(1+\beta)}\eta^5, \tag{38}$$

$$g_1 = \frac{(20N-3)(1+3\beta)}{20(1+\beta)}\eta - 3N\eta^2 + \frac{2N+\beta}{1+\beta}\eta^3 + \frac{1-3\beta}{4(1+\beta)}\eta^4 + \frac{2\beta-1}{10(1+\beta)}\eta^5, \tag{39}$$

Second-order solution:

$$h(\eta) = \sum_{m=2}^{11} a_m\eta^m, \quad k(\eta) = \sum_{m=2}^{11} b_m\eta^m, \quad f(\eta) = \sum_{m=1}^{9} c_m\eta^m, \quad g(\eta) = \sum_{m=1}^{9} d_m\eta^m, \tag{40}$$

where

$$a_2 = -\frac{1}{646800(1+\beta)^5}\{761 + 4426\beta - 149640\beta^2 + 103910\beta^3 + 607\beta^4 + 22176N^2\beta(365 + 597\beta$$

$$+1275\beta^2 + 35\beta^3) - 1848N(75 - 364\beta - 1846\beta^2 + 1300\beta^3 + 115\beta^4)\}, \tag{41}$$

$$a_3 = \frac{1}{323400(1+\beta)^5}\{-2929 + 7584\beta - 64510\beta^2 + 7584\beta^3 - 2929\beta^4 - 22176N^2\beta(-75 - 479\beta$$

$$-565\beta^2 + 175\beta^3) + 616N(-180 + 1121\beta + 3229\beta^2 + 431\beta^3 + 1095\beta^4)\}, \tag{42}$$

$$a_4 = \frac{N\beta}{70(1+\beta)^4}\{-289 - 104\beta - 247\beta^2 + 168N(15 + 16\beta + 25\beta^2)\}, \tag{43}$$

$$a_5 = \frac{1}{700(1+\beta)^4}\{32 + (-55 + 1884N - 40320N^2)\beta - 4(-19 + 36N + 21168N^2)\beta^2$$

$$+(-53 + 1716N - 60480N^2)\beta^3\}, \tag{44}$$

$$a_6 = \frac{1}{2100(1+\beta)^4}\{-113 + 237\beta - 51\beta^2 + 247\beta^3 + 40320N^2\beta(2 + 5\beta + 3\beta^2)$$

$$-42N(-15 - 17\beta - \beta^2 + 145\beta^3)\}, \tag{45}$$

$$a_7 = -\frac{3}{1225(1+\beta)^4}\{2240N^2\beta(2 + 5\beta + 3\beta^2) + 3(-3 + 4\beta + \beta^2 + 6\beta^3)$$

$$-14N(-5 - 12\beta + 89\beta^2 + 120\beta^3)\}, \tag{46}$$

$$a_8 = \frac{-3\{1 + 8(1 + 4N)\beta + (512N - 9)\beta^2\}}{560(1+\beta)^3}, a_9 = \frac{1 + (7 + 8N)\beta + (128N - 18)\beta^2}{210(1+\beta)^3}, \tag{47}$$

$$a_{10} = -\frac{2(1 + 3\beta - 13\beta^2)}{525(1+\beta)^3}, a_{11} = \frac{4(1 + 3\beta - 13\beta^2)}{5775(1+\beta)^3}, \tag{48}$$

$$b_2 = \frac{\beta}{646800(1+\beta)^5}\{-607 - 103910\beta + 149640\beta^2 - 4426\beta^3 - 761\beta^4 - 22176N^2(35 + 1275\beta$$

$$+597\beta^2 + 365\beta^3) + 1848N(115 + 1300\beta - 1846\beta^2 - 364\beta^3 + 75\beta^4)\}, \tag{49}$$

$$b_3 = \frac{\beta}{323400(1+\beta)^5}\{-2929 + 7584\beta - 64510\beta^2 + 7584\beta^3 - 2929\beta^4 + 22176N^2(-175 + 565\beta$$

$$+479\beta^2 + 75\beta^3) - 616N(-1095 - 431\beta - 3229\beta^2 - 1121\beta^3 + 180\beta^4)\}, \tag{50}$$

$$b_4 = \frac{N\beta}{70(1+\beta)^4}\{-247 - 104\beta - 289\beta^2 + 168N(25 + 16\beta + 15\beta^2)\}, \tag{51}$$

$$b_5 = \frac{\beta}{700(1+\beta)^4}\{-53+76\beta-55\beta^2+32\beta^3-4032N^2(15+21\beta+10\beta^2)$$

$$+12N(143-12\beta+157\beta^2)\}, \tag{52}$$

$$b_6 = \frac{\beta}{2100(1+\beta)^4}\{247-51\beta+237\beta^2-113\beta^3+40320N^2(3+5\beta+2\beta^2)$$

$$+42N(-145+\beta+17\beta^2+15\beta^3)\}, \tag{53}$$

$$b_7 = -\frac{3\beta}{1225(1+\beta)^4}\{2240N^2(3+5\beta+2\beta^2)+3(6+\beta+4\beta^2-3\beta^3)$$

$$+14N(-120-89\beta+12\beta^2+5\beta^3)\}, \tag{54}$$

$$b_8 = \frac{-3\beta\{-9+8\beta+\beta^2+32N(16+\beta)\}}{560(1+\beta)^3}, b_9 = \frac{\beta\{-18+7\beta+\beta^2+8N(16+\beta)\}}{210(1+\beta)^3}, \tag{55}$$

$$b_{10} = -\frac{2\beta(-13+3\beta+\beta^2)}{525(1+\beta)^3}, b_{11} = \frac{4\beta(-13+3\beta+\beta^2)}{5775(1+\beta)^3}, \tag{56}$$

$$c_1 = \frac{1}{6300(1+\beta)^3}\{320+667\beta-163\beta^2-24\beta^3-18N(515+983\beta+41\beta^2+5\beta^3)$$

$$+1260N^2(45+63\beta+7\beta^2+13\beta^3)\}, \tag{57}$$

$$c_2 = \frac{N\{59-180\beta-95\beta^2+84N(-15+58\beta+5\beta^2)\}}{140(1+\beta)^2}, \tag{58}$$

$$c_3 = \frac{16+(354N-1-17640N^2)\beta+(37-114N-20832N^2)\beta^2-24N(175N-6)\beta^3}{210(1+\beta)^3}, \tag{59}$$

$$c_4 = -\frac{1}{1680(1+\beta)^3}\{383+95\beta+49\beta^2-95\beta^3+84N(-45-149\beta-147\beta^2+5\beta^3)$$

$$-20160N^2\beta(5+7\beta+2\beta^2)\}, \tag{60}$$

$$c_5 = \frac{1}{700(1+\beta)^3}\{90 + 57\beta - 3\beta^2 - 24\beta^3 + 14N(-75 - 421\beta - 287\beta^2 + 95\beta^3)$$

$$-3360N^2\beta(3 + 5\beta + 2\beta^2)\}, \tag{61}$$

$$c_6 = \frac{-1 - 7\beta + 2N(3 + 34\beta - 23\beta^2)}{20(1+\beta)^2}, c_7 = \frac{7 + (56 - 104N)\beta + (-9 + 92N)\beta^2}{140(1+\beta)^2}, \tag{62}$$

$$c_8 = \frac{-19 - 100\beta + 33\beta^2}{560(1+\beta)^2}, c_9 = \frac{16 + 76\beta - 33\beta^2}{2520(1+\beta)^2}, \tag{63}$$

$$d_1 = \frac{1}{6300(1+\beta)^3}\{-24 - 163\beta + 667\beta^2 + 320\beta^3 - 18N(5 + 41\beta + 983\beta^2 + 515\beta^3)$$

$$+1260N^2(13 + 7\beta + 63\beta^2 + 45\beta^3)\}, \tag{64}$$

$$d_2 = -\frac{N\{95 + 180\beta - 59\beta^2 + 84N(-5 - 58\beta + 15\beta^2)\}}{140(1+\beta)^2}, \tag{65}$$

$$d_3 = \frac{\beta(37 - \beta + 16\beta^2) + 6N(24 - 19\beta + 59\beta^2) - 168N^2(25 + 124\beta + 105\beta^2)}{210(1+\beta)^3}, \tag{66}$$

$$d_4 = \frac{1}{1680(1+\beta)^3}\{95 - 49\beta - 95\beta^2 - 383\beta^3 + 84N(-5 + 147\beta + 149\beta^2 + 45\beta^3)$$

$$+20160N^2(2 + 7\beta + 5\beta^2)\}, \tag{67}$$

$$d_5 = -\frac{1}{700(1+\beta)^3}\{24 + 3\beta - 57\beta^2 - 90\beta^3 + 14N(-95 + 287\beta + 421\beta^2 + 75\beta^3)$$

$$+3360N^2(2 + 5\beta + 3\beta^2)\}, \tag{68}$$

$$d_6 = \frac{-\beta(7+\beta) + 2N(-23 + 34\beta + 3\beta^2)}{20(1+\beta)^2}, d_7 = \frac{-9 + 56\beta + 7\beta^2 - 4N(-23 + 26\beta)}{140(1+\beta)^2}, \tag{69}$$

$$d_8 = \frac{33 - 100\beta - 19\beta^2}{560(1+\beta)^2}, d_9 = \frac{-33 + 76\beta + 16\beta^2}{2520(1+\beta)^2}, \tag{70}$$

In a similar manner, the higher order terms can be obtained. But the calculations will become complicated. Moreover, the solutions considered are valid for small values of R. Therefore, we retain up to second-order terms.

From Eq. (18), the pressure drop in the z-direction can be written in non-dimensional form as follows:

$$\begin{aligned} P^* = \quad & \tfrac{p(x,y,1)-p(x,y,\eta)}{\rho U_3^2} = \tfrac{1}{2}\{(h+k)^2-1\} \\ & +\tfrac{1}{R}(h'+k') - 2N(h'+k')^2 \\ & +N\{(h+k)(h''+k'') - h''(1) - k''(1)\} \end{aligned} \tag{71}$$

It is also of interest to determine the effect of the non-dimensional elastic parameter N on the shear stresses on the elliptic plate. From Eqs. (1) – (3) and (9), we obtain

$$\begin{aligned} T_{zx} = \quad & \tfrac{U_1\eta_0}{d} f'(1) + \tfrac{k_0 U_1 U_3}{d^2} f''(1) + \tfrac{\eta_0 U_3 x}{d^2} h''(1) \\ & +\tfrac{k_0 U_3^2 x}{d^3} h'''(1), \end{aligned} \tag{72}$$

$$\begin{aligned} T_{zy} = \quad & \tfrac{U_2\eta_0}{d} g'(1) + \tfrac{k_0 U_2 U_3}{d^2} g''(1) + \tfrac{\eta_0 U_3 y}{d^2} k''(1) \\ & +\tfrac{k_0 U_3^2 y}{d^3} k'''(1) \end{aligned} \tag{73}$$

For the problem under consideration it is important to find the lift L and drag components (D_x, D_y). These physical quantities can be calculated by integrating pressure and shear stress components on the elliptic plate. The dimensionless expressions for the lift and drag are given by

$$\begin{aligned} L^* = \quad & \tfrac{4\eta_0^2}{\rho^3 U_3^4 S D^2} \int\limits_S \int (p - p_A) dS = -\tfrac{1}{R^3}(h'''(0) \\ & +RN\{h''(0)^2 - h''(0)k''(0)\}), \end{aligned} \tag{74}$$

$$D_x^* = -\frac{1}{\rho S U_1 U_3} \int\limits_S \int T_{zx} dS = -\frac{f'(1)}{R} - N f''(1), \tag{75}$$

$$D_y^* = -\frac{1}{\rho S U_2 U_3} \int\limits_S \int T_{zy} dS = -\frac{g'(1)}{R} - N g''(1) \tag{76}$$

where p_A is the ambient pressure at the edge of the elliptic plate.

Numerical results and discussion

In the present analysis, the problem of three-dimensional flow of a Walter's B' viscoelastic fluid between a porous elliptic plate and the ground discussed. As in similar studies, the governing equations were reduced to a set of ordinary differential equations by using the appropriate transformations for the velocity components. The perturbation technique was used to obtain the solution for small values of the cross-flow Reynolds number. Such solutions are very practical from both the theoretical and technological points of view. From a theoretical point of view, the effects of successive terms in the perturbation expansion decrease very rapidly. From a technological point of view, the cross-flow Reynolds numbers for currently used sliders are less than unity, as pointed out by Wang (1978).

The major axis of the elliptic slider under consideration is the segment of length $2D/\sqrt{\beta}$ between the y-intercepts $(0, \pm D/\sqrt{\beta})$. The minor axis is the segment of length $2D$ between the x-intercepts $(\pm D, 0)$. Its eccentricity $e = \sqrt{1-\beta}$, which indicates the degree of departure from circularity, may vary from 0 to 1. Note that our current results reduce the circular case when e = 0 (*i.e.*, $\beta = 1$), and the flat case when e = 1 (*i.e.*, $\beta = 0$). As a result, the perturbation solutions presented in this research include the special cases corresponding to a porous circular slider and a porous flat slider. As far as practical applications are concerned, it is important to know solutions relating to the above-mentioned special cases. With the help of Eqs. (35) to (70), these solutions are obtained as follows:

Porous flat slider:

i) Newtonian solution (cf. Skalak and Wang, 1975)

$$h_N(\eta) = 3\eta^2 - 2\eta^3 + R(\frac{8}{35}\eta^2 - \frac{27}{70}\eta^3 + \frac{3}{10}\eta^5 - \frac{1}{5}\eta^6 + \frac{2}{35}\eta^7) + R^2(-\frac{761}{646800}\eta^2 - \frac{2929}{323400}\eta^3$$

$$+\frac{8}{175}\eta^5 - \frac{113}{2100}\eta^6 + \frac{27}{1225}\eta^7 - \frac{3}{560}\eta^8 + \frac{1}{210}\eta^9 - \frac{2}{525}\eta^{10} + \frac{4}{5775}\eta^{11}) + O(R^3),$$

$$f_N(\eta) = 1 - \eta + R(-\frac{9}{20}\eta + \eta^3 - \frac{3}{4}\eta^4 + \frac{1}{5}\eta^5) + R^2(\frac{16}{315}\eta + \frac{8}{105}\eta^3 - \frac{383}{1680}\eta^4 + \frac{9}{70}\eta^5 - \frac{1}{20}\eta^6$$

$$+\frac{1}{20}\eta^7 - \frac{19}{560}\eta^8 + \frac{2}{315}\eta^9 + N(-\frac{103}{70}\eta + \frac{59}{140}\eta^2 + \frac{9}{4}\eta^4 - \frac{3}{2}\eta^5 + \frac{3}{10}\eta^6) + O(R^3),$$

$$g_N(\eta) = 1 - \eta + R(-\frac{3}{20}\eta + \frac{1}{4}\eta^4 - \frac{1}{10}\eta^5) + R^2(-\frac{2}{525}\eta + \frac{19}{336}\eta^4 - \frac{6}{175}\eta^5 - \frac{9}{140}\eta^7$$

$$+\frac{33}{560}\eta^8 - \frac{11}{840}\eta^9) + O(R^3). \tag{77}$$

ii) Viscoelastic solution (cf. Ariel, 1993)

$$h(\eta) = h_N(\eta) + R^2N(\frac{3}{14}\eta^2 - \frac{12}{35}\eta^3 + \frac{3}{10}\eta^6 - \frac{6}{35}\eta^7),$$

$$f(\eta) = f_N(\eta) + 3RN\eta(1-\eta)(1+3RN) + R^2N(-\frac{103}{70}\eta + \frac{59}{140}\eta^2 + \frac{9}{4}\eta^4 - \frac{3}{2}\eta^5 + \frac{3}{10}\eta^6),$$

$$g(\eta) = g_N(\eta) + RN(\eta - 3\eta^2 + 2\eta^3) + R^2N(-\frac{1}{70}\eta - \frac{19}{28}\eta^2 + \frac{24}{35}\eta^3 - \frac{1}{4}\eta^4 + \frac{19}{10}\eta^5$$

$$-\frac{23}{10}\eta^6 + \frac{23}{35}\eta^7) + R^2N^2(\frac{13}{5}\eta + 3\eta^2 - 20\eta^3 + 24\eta^4 - \frac{48}{5}\eta^5). \tag{78}$$

Porous circular slider:

i) Newtonian solution (cf. Wang, 1974)

$$h_N(\eta) = \frac{3}{2}\eta^2 - \eta^3 + R(\frac{13}{140}\eta^2 - \frac{9}{70}\eta^3 + \frac{1}{20}\eta^6 - \frac{1}{70}\eta^7) + R^2(\frac{26}{13475}\eta^2 - \frac{23}{4312}\eta^3 + \frac{1}{105}\eta^6$$

$$-\frac{9}{2450}\eta^7 - \frac{1}{168}\eta^9 + \frac{3}{700}\eta^{10} - \frac{3}{3850}\eta^{11}) + O(R^3), f_N(\eta) = 1 - \eta + R(-\frac{3}{10}\eta + \frac{1}{2}\eta^3 - \frac{1}{4}\eta^4 + \frac{1}{20}\eta^5)$$

$$+R^2(\frac{1}{63}\eta + \frac{13}{420}\eta^3 - \frac{9}{280}\eta^4 + \frac{3}{140}\eta^5 - \frac{1}{10}\eta^6 + \frac{27}{280}\eta^7 - \frac{43}{1120}\eta^8 + \frac{59}{10080}\eta^9) + O(R^3). \tag{79}$$

ii) Viscoelastic solution (it does not exist in the literature)

$$h(\eta) = h_N(\eta) + RN(-\frac{21}{35}\eta^2 + \frac{12}{5}\eta^3 - 3\eta^4 + \frac{6}{5}\eta^5) + R^2N(-\frac{9}{140}\eta^2 + \frac{178}{525}\eta^3 - \frac{4}{7}\eta^4$$

$$+\frac{54}{175}\eta^5 - \frac{7}{50}\eta^6 + \frac{72}{175}\eta^7 - \frac{51}{140}\eta^8 + \frac{17}{210}\eta^9) + R^2N^2(-\frac{426}{175}\eta^2 + \frac{354}{175}\eta^3 + \frac{42}{5}\eta^4 - \frac{414}{25}\eta^5$$

$$+12\eta^6 - \frac{24}{7}\eta^7), f(\eta) = f_N(\eta) + RN(2\eta - 3\eta^2 + \eta^3) + R^2N(-\frac{193}{350}\eta - \frac{27}{70}\eta^2 + \frac{8}{35}\eta^3 + \frac{21}{10}\eta^4 - \frac{43}{25}\eta^5$$

$$+\frac{7}{20}\eta^6 - \frac{3}{140}\eta^7) + R^2N^2(\frac{16}{5}\eta + \frac{36}{5}\eta^2 - \frac{127}{5}\eta^3 + 21\eta^4 - 6\eta^5). \quad (80)$$

The fact that the results presented above are in complete agreement with those obtained previously by a number authors gives us confidence regarding our algebraic calculations.

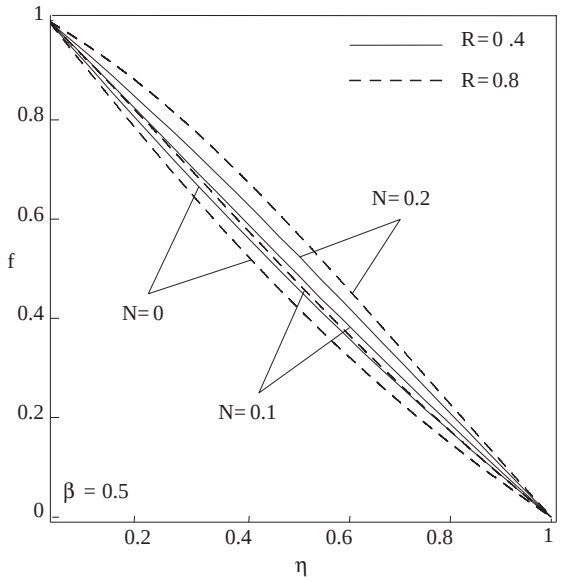

Figure 2. Lateral velocity profiles in the x direction

The predictions based on the foregoing analysis are displayed graphically for various values of the parameters in Figures 2 to 5. For a porous flat plate, the exact numerical integration shows that the perturbation solution gives acceptable results for values of R up to unity, only for small values of elastic parameter N ($\leqslant 0.2$) (Ariel, 1993). We also expect our results to be valid only for small values of R and N. For this reason, the variations of R and N are limited to the ranges 0.0 to 0.8 and 0.0 to 0.2, respectively. In addition, the effect of the eccentricity is insignificant on the velocity components and axial pressure drop at low cross-flow Reynolds numbers, so the graphs are drawn only for $\beta = 0.5$.

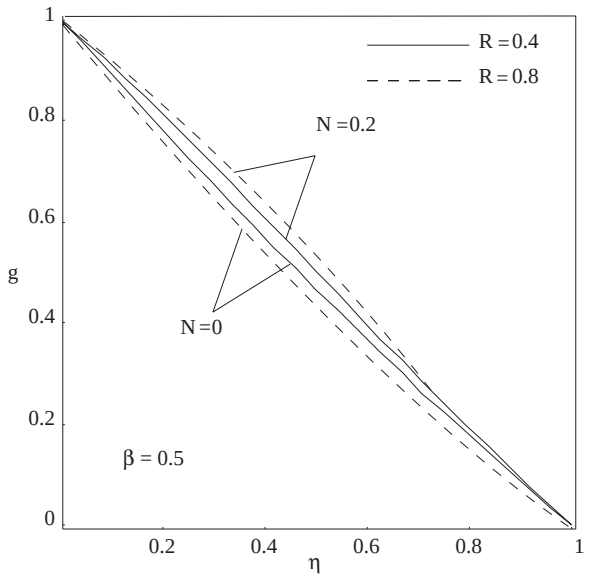

Figure 3. Lateral velocity profiles in the y direction

Figures 2 to 4 show the velocity profiles corresponding to the x, y and z directions, respectively. We observe from these figures that the elastic elements in the viscous fluid increase the lateral velocity components along the x and y axes, whereas they decrease the velocity component in the z direction slightly. These changes in the values of the velocity components are more pronounced with an increase in the cross-flow Reynolds number. Figure 5 represents

the pressure drop in the z direction for different values of R and N. From this figure, it is clear that with the decrease in the cross-flow Reynolds number, the axial pressure drop increases and the elasticity of the fluid increases it further at any point.

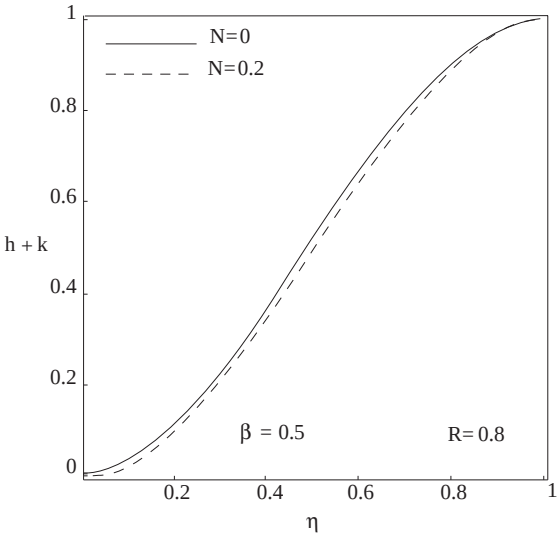

Figure 4. Vertical velocity profiles

For a porous slider, the important physical quantities are lift and drag. Table 1 illustrates the non-dimensional lift and drag components for various values of the parameters. From this table, we arrive at the conclusion that for a Newtonian and viscoelastic fluid both lift and drag increase rapidly, although at different rates, as the cross-flow Reynolds number decreases. Physically this can be explained as follows: if everything else is held fixed, the decrease in the value of the cross-flow Reynolds number results only from the decrease in the gap width. In this case, since the changes in the values of the velocity components occur in the smaller distance, velocity gradients become larger. It is for this reason that both stress components in the fluid layer and lift and drag on the porous elliptic slider increase considerably as

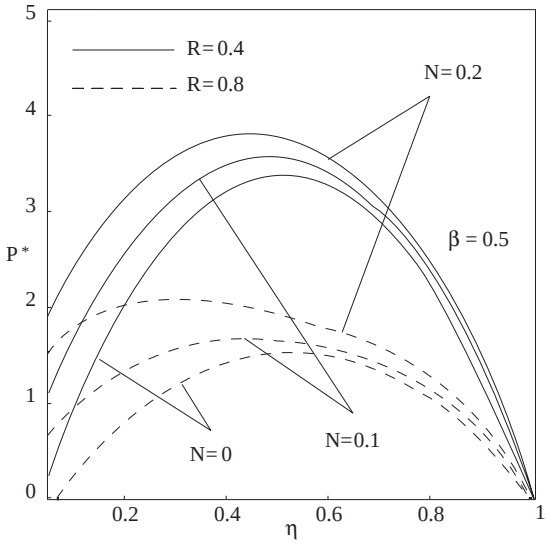

Figure 5. Axial pressure drop

Table 1. Lift and drag

		R = 0.2			R = 0.5			
β	e	L^*	D_x^*	D_y^*	L^*	D_x^*	D_y^*	N
		1558.129	4.481	4.659	105.366	1.527	1.673	0
0	1	1466.344	4.738	4.538	90.209	1.720	1.533	0.1
		1374.460	5.053	4.413	74.945	2.055	1.412	0.2
		1289.430	4.510	4.628	86.344	1.550	1.645	0
0.2	0.894	1220.750	4.704	4.571	74.887	1.687	1.563	0.1
		1150.910	4.943	4.514	63.053	1.934	1.497	0.2
		1027.320	4.539	4.598	68.414	1.573	1.619	0
0.5	0.707	975.992	4.670	4.604	59.738	1.655	1.593	0.1
		923.280	4.833	4.618	50.577	1.815	1.594	0.2
		855.068	4.559	4.578	56.853	1.588	1.604	0
0.8	0.447	813.162	4.648	4.626	49.725	1.634	1.613	0.1
		769.956	4.761	4.689	42.101	1.739	1.665	0.2
		769.446	4.568	–	51.149	1.596	–	0
1	0	731.822	4.637	–	44.740	1.623	–	0.1
		692.984	4.724	–	37.845	1.701	–	0.2

Table 2. Coefficients of sliding friction

		R = 0.2		R = 0.5		
β	e	μ_x	μ_y	μ_x	μ_y	N
0	1	0.00287	0.00299	0.01449	0.01587	0
		0.00323	0.00309	0.01906	0.01699	0.1
		0.00367	0.00321	0.02742	0.01884	0.2
0.2	0.894	0.00349	0.00358	0.01795	0.01905	0
		0.00385	0.00374	0.02252	0.02087	0.1
		0.00429	0.00392	0.03067	0.02374	0.2
0.5	0.707	0.00418	0.00447	0.02299	0.02366	0
		0.00478	0.00471	0.02770	0.02666	0.1
		0.00523	0.00500	0.03588	0.03151	0.2
0.8	0.447	0.00533	0.00535	0.02793	0.02821	0
		0.00571	0.00568	0.03286	0.03243	0.1
		0.00618	0.00608	0.04131	0.03954	0.2
1	0	0.00593	–	0.03120	–	0
		0.00633	–	0.03627	–	0.1
		0.00681	–	0.04494	–	0.2

the cross-flow Reynolds number decreases. On the other hand, for a Newtonian fluid, the lift is of order R^{-3} whereas the drag components are of order R^{-1} (see Eqs. (74)-(76)). Thus, the coefficients of sliding friction, namely μ_x and μ_y, in the x- and y-directions, which are respectively defined as D_x^*/L^* and D_y^*/L^* ratios, are proportional to R^2. Since it is aimed to reduce the frictional resistance in the x- and y-directions for a porous slider, the ratio of drag to lift must be made very small. In light of this argument, Table 2 leads us to conclude that the fact that the porous sliders should be operated at small values of cross-flow Reynolds number still remains valid even when a viscoelastic fluid is used. Again from Table 2, in the case of Newtonian fluid, we notice that the ratio of drag to lift in the x direction increases with the decrease in the eccentricity, and that $\mu_x < \mu_y$. Hence, as far as optimum efficiency is concerned, it is more advantageous to move an elliptic slider with high eccentricity along the minor axis. Contrary to the Newtonian fluid, for a viscoelastic fluid, it is more efficient to move an elliptic slider with high eccentricity along the major axis.

Conclusions

In this paper, we are concerned with a theoretical investigation of the steady three-dimensional flow of a Walter's B' viscoelastic fluid between a porous elliptic plate and the ground. By means of appropriate similarity transformations, the governing equations are reduced to a set of ordinary differential equations. Approximate solutions to these equations are obtained by employing a perturbation method taking the cross-flow Reynolds number as a perturbation parameter. The graphical and tabular presentation of the results reveals the effect of the elasticity of the fluid on the velocity distribution, and axial pressure drop as well as lift and drag. Some of the qualitatively interesting conclusions which can be drawn from this analysis are summarized as follows:

1. The elasticity of the fluid increases the lateral velocity components, whereas it decreases the axial velocity component.

2. The above-mentioned changes in the velocity components are more noticable for the case of a large cross-flow Reynolds number.

3. Axial pressure drop increases with the decrease in cross-flow Reynolds number and the elastic elements in the viscous fluid increase it further at any point.

4. The effect of the eccentricity is insignificant on the velocity components and axial pressure drop at low cross-flow Reynolds numbers.

5. For both Newtonian and viscoelastic fluids, porous sliders should be operated at small values of cross-flow Reynolds number with a view to reducing the coefficients of sliding friction in the lateral directions.

6. From the optimum efficiency point of view, for a Newtonian fluid it is more advantageous to move an elliptic slider with high eccentricity along the minor axis, whereas in the case of viscoelastic fluid, to move it along the major axis.

Acknowledgement

The author is grateful to the referees whose comments and suggestions improved the presentation and value of the paper.

Nomenclature

d	distance between the elliptic plate and the ground, L
D_x, D_y	drag components , MLT^{-2}
D_x^*, D_y^*	nondimensional drag components
e	eccentricity, dimensionless
$\mathbf{e}$	rate of strain tensor, T^{-1}
$\mathbf{I}$	identity tensor, dimensionless
k_0	short memory coefficient, ML^{-1}
L	lift , MLT^{-2}
L^*	non-dimensional lift
N	elastic number, dimensionless
p	pressure, $ML^{-1}T^{-2}$
p_A	ambient pressure, $ML^{-1}T^{-2}$
P^*	axial pressure drop, dimensionless
R	cross-flow Reynolds number, dimensionless
$\mathbf{T}$	Cauchy stress tensor, $ML^{-1}T^{-2}$
t	time, T
U_1, U_2	constant lateral velocity components, LT^{-1}
U_3	uniform injection velocity, LT^{-1}
u, v, w	components of the velocity vector, LT^{-1}
$\mathbf{v}$	velocity vector, LT^{-1}
β	square of the ratio of minor axis to major axis, dimensionless
η	normalized axial coordinate, dimensionless
η_0	limiting viscosity at small rate of shear, $ML^{-1}T^{-1}$
μ_x, μ_y	coefficients of sliding friction, dimensionless
ρ	density, ML^{-3}
τ	relaxation time, T

References

Ariel, P.D., "Flow of Viscoelastic Fluids through a Porous Channel - I", Int. J. Numer. Methods Fluids, 17, 605-633, 1993.

Bhatt, B.S., "The Elliptic Porous Slider at Low Cross-Flow Reynolds Number Using a Non-Newtonian Second-Order Fluid", Wear, 71, 249-253, 1981.

Brady, J.F., "Flow Development in a Porous Channel and Tube", Phys. Fluids, 27, 1061-1067, 1984.

Beard, D.W. and Walters. K., "Elastico-Viscous Boundary Layer Flows. Part I. Two-Dimensional Flow near a Stagnation Point", Proc. Camb. Phil. Soc., 60, 667-674, 1964.

Berman, A.S., "Laminar Flow in Channels with Porous Walls", J. Appl. Phys., 24, 1232-1235, 1953.

Choi, J.J., Rusak, Z. and Tichy, J.A., "Maxwell Fluid Suction Flow in a Channel", J. Non-Newtonian Fluid Mech., 85, 165-187, 1999.

Cox, S.M., "Two Dimensional Flow of a Viscous Fluid in a Channel with Porous Walls", J. Fluid Mech., 227, 1-33, 1991.

Proudman, I., "An Example of Steady Laminar Flow at Large Reynolds Number", J. Fluid Mech., 9, 593-602, 1960.

Sellars, J.R., "Laminar Flow in Channels with Porous Walls at High Suction Reynolds Number", J. Appl. Phys., 26, 489-490, 1955.

Skalak, F.M. and Wang, C.Y., "Fluid Dynamics of a Long Porous Slider", J. Appl. Mech. Trans. ASME, 42, 893-894, 1975.

Skalak, F.M. and Wang, C.Y., "On the Nonunique Solutions of Laminar Flow through a Porous Tube or Channel", SIAM J. Appl. Math., 34, 535-544, 1978.

Terrill, R.M. and Shrestha, G.M., "Laminar Flow through Parallel and Uniformly Porous Walls of Different Permeability", J. Appl. Math. Phys. (ZAMP), 16, 470-482, 1965.

Wang, C.Y., "Fluid Dynamics of the Circular Porous Slider", J. Appl. Mech. Trans. ASME, 41, 343-347, 1974.

Wang, C.Y., "The Elliptic Porous Slider at Low Crossflow Reynolds Numbers", J. Lubrication Technol. Trans. ASME, 100, 444-446, 1978.

Watson, L.T., Li, T.Y., Wang, C.Y., "Fluid Dynamics of the Elliptic Porous Slider", J. Appl. Mech. Trans. ASME, 45, 435-436, 1978.

White, F.M., Barfield, B.F., Goglia, M.J., "Laminar Flow in a Uniformly Porous Channel", J. Appl. Mech. Trans. ASME, 25, 613-617, 1958.

Yuan, S.W., "Further Investigation of Laminar Flow in Channels with Porous Walls", J. Appl. Phys. 27, 267-269, 1956.

Zaturska, M.B., Drazin, P.G., Banks, W.H.H., "On the Flow of a Viscous Fluid Driven along a Channel by Suction at Porous Walls", Fluid Dyn. Res., 4, 151-178, 1988.